

Artificial Color Contrast for Machine Vision and its Effects on Feature Detection

Kok-Meng Lee*, Wayne Daley and Qiang Li

Abstract— Color information is useful in vision-based feature detection, particularly for applications involving natural objects. One of the factors influencing the success rate of color machine vision in detecting a target is its ability to characterize the color. When unrelated features are very close to the target in the color space, which may not pose a significant problem to an experienced operator, they appear as noise and often result in false detection. This paper describes a method for creating artificial color contrast (ACC) between features in color space with objective of highlighting the target while suppressing surrounding noise; the development of this ACC method has been motivated by the ability of the human to perceive fine gradation of a variety of color especially for natural products where, in most cases, humans are still the sensor of choice. The efficiency of this method is demonstrated on representative automation problems.

Keywords— Machine Vision, Inspection, color classification

I. INTRODUCTION

Machine vision (MV) has been applied extensively in many automated inspection tasks. As compared to humans, MV can make more accurate quantitative measurement and has been successfully employed for gauging man-made objects designed to definable tolerances. Early MV research has largely focused on developing algorithms that use edge and shape information of grayscale images to make decisions. Their applications to high-speed automation of natural products, such as food-processing or agricultural live-object handling where reliability, cycle time and productivity are of prime concern and variability in natural objects is usually several orders-of-magnitude higher than that for manufactured goods, have remained a challenge. As a result, most solutions to inspection problems of natural product today still have humans in the loop. MV algorithms that can provide robust sensing of natural product at high speed would be of tremendous value since MV systems do not get tired and suffer performance degradation as a result, and can free many of the people now conducting these jobs for more constructive activity.

The presence of color is one of the most striking

features in nature. Over the past two decades, an increase in color MV (CMV) research has been seen in industry and space exploration as well as in human face identification. This trend appears to be accelerating because of the rapid advance in digital vision sensor technology coupled with the lucrative market of consumer color cameras, which continues to lower the cost of color vision hardware. In addition, color information is an attractive addition to edge and shape, particularly for food processing applications where color variability often renders grayscale-based MV algorithms difficult or impossible to work. Figures 1(a) and 2(a) show two sample examples with inspection problems commonly encountered in food processing [1] [2]; grapefruit inspection and detection of contamination in packaged food product, where MV is used to sort this product based on user generated parameters. Figures 1(b) and 2(b) show the grayscale images of the same two products; it can be seen that color is necessary in order to differentiate between defective areas (such as the blush or contamination) as they would be confused with shading. Figures 1(c) and 2(c) show the transformed images (that are more desired representation to machines) using a technique discussed in this paper, where color contrast between features is artificially created while noise is suppressed.

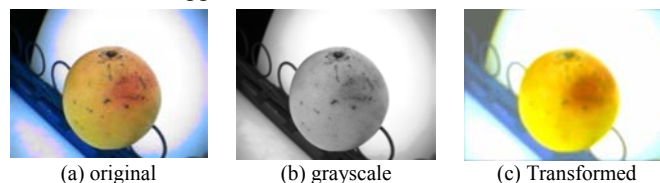


Fig. 1 Grapefruit inspection

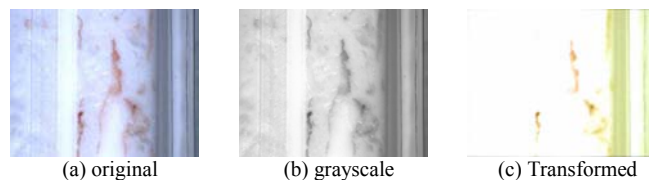


Fig. 2 Detection of contaminations in packaged food

However, CMV has its own problems. One of the factors influencing the success rate of a CMV in detecting a target is its ability to characterize color [3]. The boundary of the patterns characterizing the target in color space (for practical automation) can only be constructed from a limited set of training data and thus is essentially an approximation. When unrelated features are very close to the target in color space, which may not pose a problem to an experienced operator, they appear as noise and often result in false detection. This ability of the human to perceive fine gradation of color has motivated us to develop a robust method to improve CMV reliability in finding color features

Manuscript received March 1, 2005. This work was supported in part by the Georgia Agricultural Technology Research Program (ATRP) and the U.S. Poultry and Eggs (USPE) Association.

*Corresponding author-K.-M. Lee, Professor, Woodruff School of Mechanical Engineering, Georgia Institute of Technology, Atlanta, Georgia 30332-0405, USA (e-mail: kokmeng.lee@me.gatech.edu)

W. Daley, Senior Research Engineer, Georgia Tech Research Institute, Atlanta, GA 30332, USA (e-mail: wayne.daley@gtri.gatech.edu)

Q. Li, Ph.D. Candidate, Woodruff School of Mechanical Engineering, Georgia Institute of Technology, Atlanta, Georgia 30332, USA (e-mail: gtg873k@mail.gatech.edu)

in natural product, which partially emulates some functions in human visual system (HVS) by creating ACC.

Color vision has been extensively studied for two centuries and has made great progress in applying in diagnosis of eye disease [4]. This knowledge leads to some understanding of color contrast (a ratio of the incremental intensity to the background illumination), which enormously enhances our visual capabilities in discriminating features from their background. Much of these visual capabilities occur in the eye (analogous to a camera) and the retina (like a signal filtering system) before reaching the brain, which we refer here on as the human visual system (HVS). In this paper, we describe a method to create ACC between features in order to reduce noise for color classification by highlighting targets while suppressing unrelated features

The understanding of the HVS models for use in solving MV problems has been actively pursued by a number of researchers during the last three decades. In the early computational vision, Marr [5] modeled vision as a process to produce from images of the external world a 3D description that is useful to the viewer. In another human performance (HP) based approach, Doll *et. al* [6] developed the Georgia Tech Vision (GTV) model for detecting texture in natural images and for tracking of tanks and faces in moving image sequences. Gershon [7] used biological models for early chromatic visual processing and for determining material changes. In [8], non-linear filters based on HVS models for smoothing images while preserving edges were found to yield performance comparable to other established techniques. There were also thoughts given towards implementing HVS models in hardware [9] [10]. These models, which assumed only achromatic information and utilized the Gaussian-based filters as representing some of the lower level operations conducted in early vision, were able to simulate some of the known behaviors on the HVS. HVS-based models have also been used in image processing (e.g. texture segmentation [11] and automating analysis of large image sets from planetary exploration [12]. More recently, Daley [2] proposed an approach for developing MV algorithms through the use of HVS models.

While our proposed solution has been motivated by HVS, we also recognize that HVS does not exhibit perfect color constancy [13] [14] and also performs poorly in lighting with abnormal spectral content (e.g. sodium arc) particularly when colors are very similar. Thus, we develop here a robust method combining the *quantitative* ability of a CMV to discriminate very small color difference between similar features, and the *qualitative* ability of a HVS to create ACC for subsequent color classification. Unlike research on color constancy that refers to the lack of change in the perceived color of a colored patch as the global illumination changes, we focus on contrast due to the change in perceived color of a colored patch as its local surround is changed given the illumination.

The remainder of this paper offers the following:

- 1) We highlight the elements in the HVS that influences color contrast pre-processing algorithms for MV-based color classification.

- 2) We provide a general formulation that uses the difference-of-Gaussians (*DoG*) for creating contrast between features in color space so that unrelated features (appearing as noise in color classification) can be more easily removed.
- 3) We examine the effects of ACC on color classification in the context of food processing and natural object handling automation applications, where variability in natural objects is usually several orders-of-magnitude higher than that for man made objects.

II. HINTS FROM HVS MODELS ON COLOR CONTRAST

In the typical HVS (Fig. 3), the cornea and lens together focus images on the retina that is part of the central nervous system. There are five types of neurons in a HVS; photoreceptors, and bipolar, ganglion, horizontal and amacrine cells. The photoreceptors (rods and cones) respond to light and transform this radiant energy into electrical activity, which is transmitted to retinal bipolar cells and then retinal ganglion cells (RGC) that output a spike train. Two other neurons, the horizontal and amacrine cells, intervene laterally in this pathway and modulate the light input. Visual processing stream flows from the eyes through the lateral geniculate nucleus, and up to the cortex where visual information is disseminated to both exclusively visual centers and other areas where it is integrated with memory and other senses. Although the visual cortex processes much information (such as form, contrast, location, movement and color of the objects being perceived), we are particularly interested in biologically inspired contrast and color since MV generally outperforms human in gauging quantitative information such as location and movement.

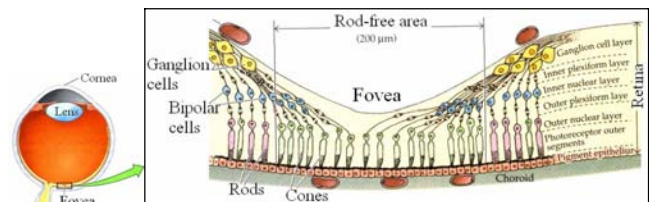


Fig. 3 Retinal neurons: photoreceptors, bipolar and ganglion cells (RGC)

A. RGC's Responds to an Edge Stimulus

Ganglion receptive fields in the eye respond to contrast. Attempts to model the contrast of a HVS led several scientists to record the firing rate of RGC that provide the sole connecting link between the *receptive* mechanisms of the retina and the more central *analyzing* mechanism of the visual system. In early 1953 Kuffler [15] combined the use of microelectrodes for recording directly from RGC bodies in the intact eye of the cat with the simulation of the retinal with localized spots of light. Among Kuffler's important findings, he found two kinds of ganglion cells, which he called ON-center and OFF-center cells for those excited and inhibited by light in the center of their receptive fields respectively. Studies for dogs' RGC have been confirmed in the cat, and it is now believed that many of the basic anatomical and physiological principles evident in the cat retina also hold for the primate retina [16].

In an attempt to provide a better understanding of the role of the retina in spatial vision, Enroth-Cugell and Rodson [17] built upon Kuffler's method and quantitatively recorded

the activities of an individual cell with a micro-electrode either directly on the soma of the cell or from the axon of the cell as it runs in the optic tract towards its central destination. In addition, they used sinusoidal gratings generated on a CRT screen as visual stimuli to develop a quantitative description of RGC behaviors using frequency response techniques. Three of Enroth-Cugell and Rodson's important findings of interest here were the following:

1. Equal and opposite effects on a RGC's firing rate can be reproduced by independent stimulation of the center and surround of its receptive field.
2. If the illumination over the entire center and surround are changed simultaneously, there is only a small transient effect on the cell's firing rate. Ganglion cells respond best to spatial patterns that cause the receptive center to be illuminated at a different level from the surround.
3. Their measurements of the RGC's firing rate as an edge was passed through the field of view of a cat are reproduced in Fig. 4(b). They modeled the RGC spatial-frequency responsibility function and receptive field weighting function as the difference of two Gaussian (*DoG*) functions. In Fig. 4(b), the smooth curve (solid line) is the fitting *DoG* on measurements (in dots) and the little pictures at the top attempt to show the spatial relationship of the stimulus pattern to the RGC's receptive field for several different spatial position.

The response (Fig. 4) shows that the striking ability of a HVS to emphasize the edge while simultaneously smooths its surround and maintain the level of contrast.

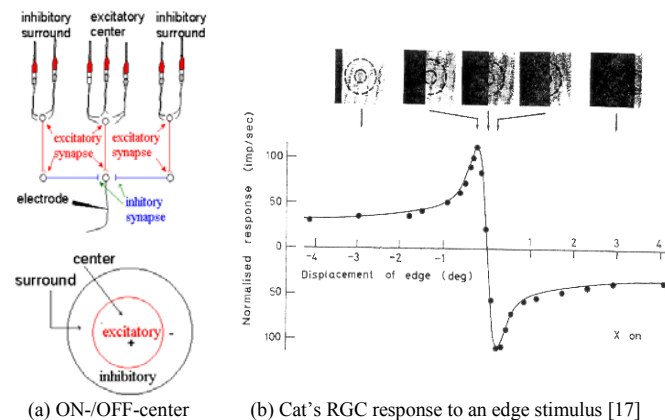


Fig. 4 Receptive field and ganglion Cell

B. Modern Models of Color Vision

There are two types of photoreceptors, rods and cones. Rods have very low spatial resolution, but extremely sensitive to light allowing us to see at night in starlight conditions. Cones, on the other hand, are relatively insensitive to light but responsible for our color vision and have high spatial resolution. The trichromacy theory tells us that our color vision comes from three types of cone cells corresponding to red-green-blue (*RGB*) or Long-Medium-Short (*LMS*) wavelengths. It, however, does not address the manner in which this information is handled beyond the photoreceptors. The opponent-colors theory of color vision, proposed by Hering [18], advanced to explain various phenomena that could not be adequately accounted for by trichromacy. Examples of such phenomena are the after-

image effect (if the eye is adapted to a yellow stimulus the removal of the stimulus leaves a blue sensation or after-effect) and the non-intuitive fact that an additive mixture of red and green light gives yellow and not a reddish-green. These and similar observations led Hering to propose the opponent color vision theory that color is processed by bipolar hue channels referred to as the red-green and blue-yellow channels. By bipolar we mean that, at any instant, each channel can signal only one of the two attributes it is capable of coping as illustrated in Fig. 5. Hering proposed that yellow-blue and red-green represent opponent signals; this also explain why there were four psychophysical color primaries red, green, yellow, and blue and not just three. Hering also proposed a white-black opponency but this third opponent channel has been abandoned in most modern versions of the theory. It is now accepted that the physiology of color vision to date established two facts:

- 1) Color vision is normally trichromatic.
- 2) Opponent processing plays a central role in coding color information.

Both the *trichromatic* and *opponent-color* theories describe essential features of our color vision with the latter theory describing the perceptual qualities of color vision that derive from the neural processing of the receptor signals in two opponent channels and a single achromatic channel.

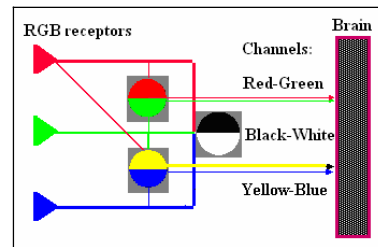


Fig. 5 Hering's theory of opponent color

III. MODEL FOR ARTIFICIAL COLOR CONTRAST

Consider a two-dimensional (2D) symmetric (zero-mean uncorrelated) Gaussian kernel:

$$G_{\sigma}(x, y) = \frac{1}{\sqrt{2\pi\sigma^2}} \exp\left(-\frac{x^2 + y^2}{2\sigma^2}\right) \quad (1)$$

to get

$$g(x, y) = G_{\sigma} * f(x, y) \quad (2)$$

where for simplicity G_{σ} denotes $G_{\sigma}(x, y)$. Similar to Laplace of a Gaussian, the image is first smoothed with the Gaussian kernel of width σ . The difference of two Gaussian-smoothed images can be written as

$$h_i(x, y) = G_{\sigma_c} * f_i(x, y) - G_{\sigma_s} * f_j(x, y) \quad (3)$$

A. DoG as an Edge-finder of a Single Grayscale Image

The difference of two Gaussians is commonly used in MV to detect edges in a grayscale image, for which $f_i(x, y) = f_j(x, y) = f(x, y)$. Thus,

$$h(x, y) = (G_{\sigma_c} - G_{\sigma_s}) * f(x, y) = DoG * f(x, y) \quad (4)$$

where the subscripts "c" and "s" denote center and surround of the excitatory and inhibitory receptive fields (Fig. 6) respectively; $\sigma_c < \sigma_s$; and the *DoG* as an operator or convolution kernel is defined as

$$DoG \triangleq G_{\sigma_c} - G_{\sigma_s} = \frac{1}{\sqrt{2\pi}} \left[\frac{1}{\sigma_c} e^{-(x^2+y^2)/2\sigma_c^2} - \frac{1}{\sigma_s} e^{-(x^2+y^2)/2\sigma_s^2} \right] \quad (5)$$

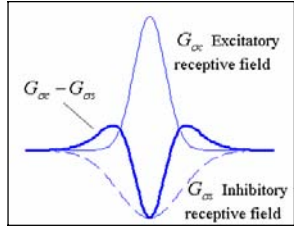


Fig. 6 DoG model of receptive field

B. Artificial Color Contrast for Feature Discrimination

To facilitate the following discussion, we broadly divide the surrounds into two types:

$$\text{Type I: } h_i(x, y) = DoG * f_i(x, y) \quad (6a)$$

$$\text{Type II: } h_j(x, y) = G_{\sigma_c} * f_i(x, y) - G_{\sigma_s} * f_j(x, y) \quad (6b)$$

Type I is essentially an edge detection filter applied on a color component. Type II allows for $f_i(x, y) \neq f_j(x, y)$. In both Types I and II, $f_i(x, y)$ with $(i=1, 2, 3)$ corresponds to *RGB* component images respectively; and $f_j(x, y)$ with $(j=4, 5, 6)$ are some linear combinations of *RGB* component images to be designed. The ACC method is to find

$$f_j(x, y) = \sum_{i=1}^3 \alpha_i f_i(x, y) \quad (7)$$

where α_i are weighting factors such that contrast between different features with similar color can be amplified artificially while retaining their edge information. We mimic the HVS by denoting the component $f_i(x, y)$ as center and the linear combination as a surround. In the subsequent discussion, we denote (for simplicity) the component images

$$R=R(x, y), G=G(x, y) \text{ and } B=B(x, y).$$

One possible set of surrounds (inspired by the Herring's opponent color theory, Fig. 5) is the R-G and Y-B channels:

$$f_{\pm(R-G)}(x, y) = \pm(R - G) \quad (8a)$$

$$f_{\pm(Y-B)}(x, y) = \pm(R + G - B) \quad (8b)$$

Their effect on colors can be seen by applying (8a) and (8b) on a color calibration pattern in Fig. 7. Much like Herring's opponent cells, $f_{R-G}(x, y)$ excites red and inhibits green. Similarly, $f_{Y-B}(x, y)$ excites yellow and inhibits blue.

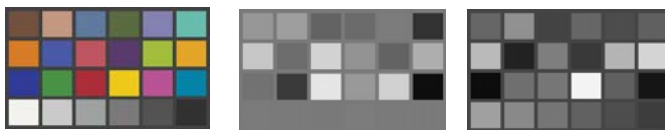


Fig. 7 Effect of R-G and Y-B channels on monitor color test patterns

Substituting (8a) into Type II,

$$h_{R_c(R-G)}(x, y) = DoG * R + G_{\sigma_s} * G \quad (9a)$$

$$h_{G_c(R-G)}(x, y) = DoG * G + G_{\sigma_s} * [2G - R] \quad (9b)$$

$$h_{B_c(R-G)}(x, y) = DoG * B + G_{\sigma_s} * [B - (R - G)] \quad (9c)$$

and similarly (8b) into Type 2,

$$h_{R_c(Y-B)}(x, y) = DoG * R + G_{\sigma_s} * [B - G] \quad (10a)$$

$$h_{G_c(Y-B)}(x, y) = DoG * G + G_{\sigma_s} * [B - R] \quad (10b)$$

$$h_{B_c(Y-B)}(x, y) = DoG * B + G_{\sigma_s} * [2B - (R + G)] \quad (10c)$$

In (9) and (10), each transformed component consists of two parts: the 1st part corresponds to Type I which essentially applies the *DoG* filter on each of the *RGB* component images and thus allows the detection of edges in the image. The 2nd part emphasizes or reduces the influences of certain color components (relative to the target color) in order to create the needed artificial contrast. The ACC method is best illustrated with examples. Due to page limitations and without loss of generality, we consider here primarily food-processing applications, where red is often a dominant feature color to be identified. Thus, we choose (8a) as the surround for the *red* and *green* component images and (8b) as the surround for the *blue* component image; the intent is to highlight red features in the background of yellow. The widths, $\sigma_c=1$ and $\sigma_s=10$ pixels, are used in the remainder of this paper. The transformed ACC space is given by (11):

$$h_4(x, y) = h_{R_c(R-G)}(x, y) = DoG * R + G_{\sigma_j} * G \quad (11a)$$

$$h_5(x, y) = h_{G_c(R-G)}(x, y) = DoG * G + G_{\sigma_s} * [2G - R] \quad (11b)$$

$$h_6(x, y) = h_{B_c(Y-B)}(x, y) = DoG * B + G_{\sigma_s} * [2B - (R + G)] \quad (11c)$$

Example 1: ACC's Effect on Contrast and Edge

Consider the test image as shown in Fig. 8(a), which made up of two similar red features with their RGB values are given in the square brackets. Figure 8(b) shows the transformed ACC image, where an offset of 100 is added to the transformed image to allow for visual illustration. Figures 8(c) and 8(d) plot the 1st and 2nd terms of (11) across the edge of the transformed image shown in 8(b). Two observations are worthy of mentioning:

- 1) The ACC method has a significant effect on enhancing contrast (denoted by the ratio $\Delta I/I$ where ΔI is the Euclidean distance between the two feature colors), which increases from 0.15 to 0.57.
- 2) Type II response, as given by the component sum in 8(a) and 8(b), resembles the cat's RGC response to an edge stimulus shown in Fig. 4 [17].

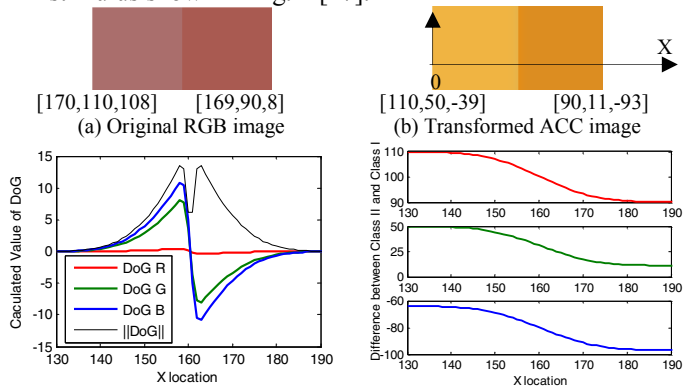


Fig. 8 Example illustrating the basic concept of ACC

Example 2: Effect of ACC to Color Classification

Figure 9(a) shows an image of a white-feathered broiler (meat chicken) on a moving conveyor, where the red comb is to be identified and the featherless spot with shadow is a potential noise. Figure 9(b) shows a representative set of

training data for classification, where two clusters (denoted by red and blue) are color pixels of the target and noise in RGB color space. These clusters (both dominant in red) are very close to each other in the color space; it makes color-based identification a difficult task. Thus, we apply the ACC method to artificially increase the separation between the two clusters. Figure 9(c) shows the transformed ACC image computed using (11a), (11b) and (11c).

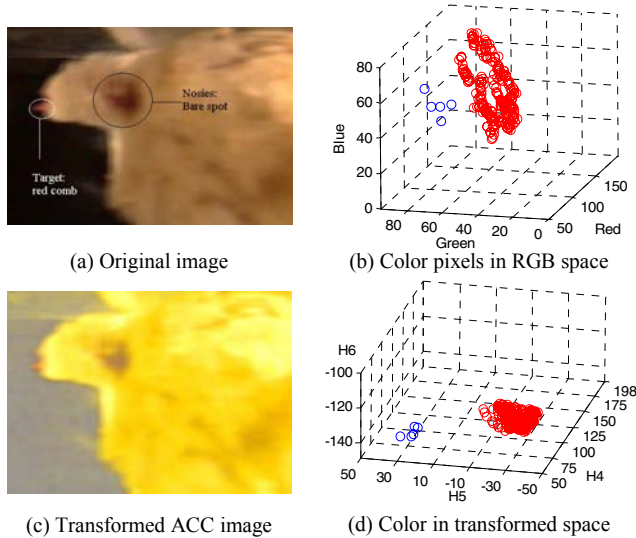


Figure 9 Comparison showing ACC's effect on features in color space

Table 1 Comparison between features in RGB and ACC transformed space

	Original: [target]/[noise]	Transformed: [target]/[noise]
Mean	[152, 58, 45]/[135, 85, 39]	[61, -34, -123]/[81, 29, -143]
SD	[3.9, 7.2, 22.2]/[1.1, 4.3, 10]	[3.5, 4.2, 12.8]/[0.5, 1.9, 7.5]
Distance	36	69

The effect of the ACC on color representation can be illustrated by comparing the pixel clusters of the original RGB image and those of the transformed ACC image in Figs. 9(b) and 9(d) respectively along with their means, standard deviation (SD), and distance in Table 1, where the SD is calculated along the principal axes. The distance between the clusters in ACC space is twice that in the RGB space. In addition, the application of the Gaussian smoothing filters results in more closely packed clusters. Both these effects will ease the design of the classifier.

IV. ILLUSTRATIVE APPLICATIONS IN FOOD PROCESSING

In this example, we illustrate the applicability of the ACC method with some real world industrial problems:

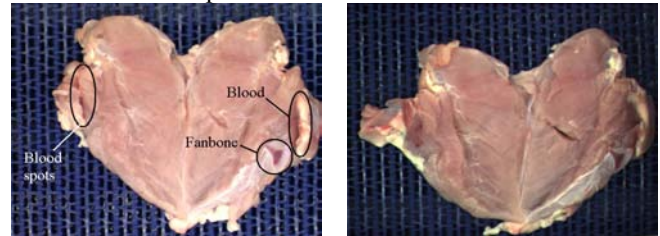
Example 1: Fanbone detection

We examine the ACC robustness to sensor resolution with a bone detection application; detection of bones in deboned product is great importance to many producers because of food safety concerns. Figures 10(a) and 11(a) show two images of a poultry (breast-butterfly) meat taken using two different color cameras:

- 1) High-resolution 3-CCD camera (Sony DXC900).
- 2) Low-cost single-chip camera (Point Grey Firefly).

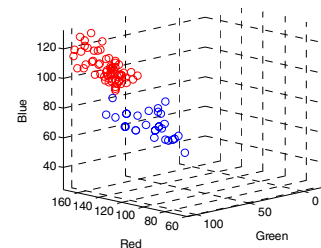
In Figs. 10(a) and 11(a), a "fan-bone" to be identified can be seen at the lower right corner on the surface. In addition, there are blood stains near the fan-bone and on the opposite side of the breast-butterfly. These blood stains, which are acceptable from a safety viewpoint, could trigger false

detection. The potential problems presented by noisy blood stains can be seen in the color patterns in the RGB space in Figs. 10(b) and 11(b); particularly in the image captured by the single-chip camera. Figures 10(c) and (d) show that ACC can effectively reduce the pixel distribution of the fanbone and blood stains in color space. It also increases the separation between the two color clusters. It is worth noting that the pre-processed image of the single-chip camera with ACC outperforms the 3-CCD image without ACC, implying that ACC could present a potentially low-cost solution to color classification problems.



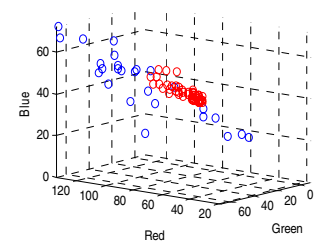
10(a) Fanbone (3-CCD)

11(a) Fanbone (single-CCD)



10(b) Color in RGB space (3-CCD)

Mean=[150, 92, 108] / [138, 62, 67]
SD=[4.1, 6.6, 11.9] / [5.3, 8.0, 14.0]
Distance= 52



11(b) Color in RGB space (1-CCD)

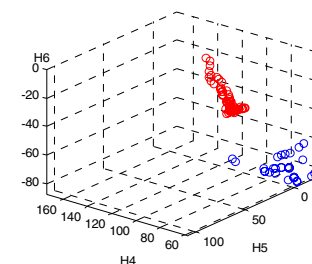
Mean=[67, 39, 44] / [93, 45, 45]
SD=[1.2, 2.3, 9.2] / [5.6, 9.9, 31.2]
Distance= 27



10(c) ACC image (3-CCD)

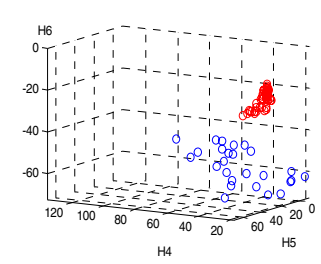


11(c) ACC image (single-CCD)



10(d) Color in ACC space (3-CCD)

Mean=[88, 30, -24] / [70, -5, -77]
SD=[1.9, 4.1, 10.9] / [4.4, 7.1, 11.9]
Distance= 67



11(d) Color in ACC space (1-CCD)

Mean=[36, 9, -24] / [50, 7, 57]
SD=[0.6, 2.0, 5.9] / [5.1, 7.8, 18.4]
Distance= 36

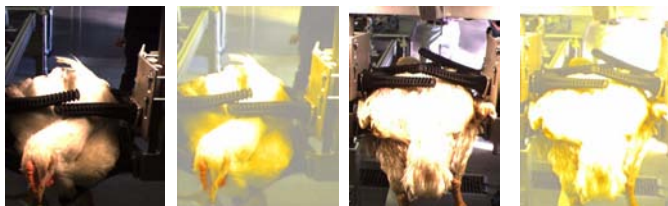
Fig. 10 Image with 3-CCD camera
SONY DXC900, 10bit, 768(H)x494(V)

Fig. 11. Single-CCD color image
Point Grey Firefly, 8-bit 640(H)x480(V)

Example 2: Live-bird Handling Application

We evaluate the effect of the ACC in the context of an automaton problem, where the bird's orientation (facing forward or backward) must be determined in real time. Specifically, we use two color classification algorithms to find the red comb of the bird as shown in Fig. 12; the RCE

neural network classifier (RCE-NNC) [19] [20] uses hyper-spheres while the support vector machine SVM [21] uses hyper-planes. These algorithms for the orientation detection problems are given in [3]. In both algorithms, morphological operation based on the rule of majority (10 pixels out of a 8x8 mask) is used as a post-processor to remove isolated pixels. The results of the color classification (with 81 640x480 color images of birds) with/without pre-processed using the ACC method are summarized in Table 2. Resulting features detected by RCE network were found to contain considerable amount of noise while the SVM tends to exclude pixels belonging to the target. Both these methods, when they are applied using the original RGB images, result in many false detection particularly in finding backward birds, for which the detection algorithm must find no feature color in the image. The ACC significantly improves the success rate of detecting the backward facing birds by increasing the distance between different features in color space.



(a) Forward without/with ACC (b) Backward without/with ACC
Fig. 12 Sample images of forward and backward facing birds

Table 2 Classification results

Algorithms	RGB images		ACC Transformed	
	Forward	backward	Forward	backward
RCE-NNC	51/51	0/30	51/51	18/30
SVM	30/51	21/30	30/51	30/30

V. CONCLUSION

A pre-processing method to enhance contrast between features in color space has been introduced. This method, inspired by the ability of human to perceive fine gradation of color, emulates the lower-level biological operation of a HVS to artificially create contrast between features while suppress noise. The effect of the ACC on color classification is essentially to increase the separation between clusters of feature pixels in color space, thereby minimizing the appearance of unrelated features as noise.

The ACC method has been evaluated in the context of MV-based food processing applications. Two commonly used color classification algorithms have been employed in the color detection for an automated live-object handling problem. When the color classification is applied on the original RGB images, both these methods result in much false detection. We demonstrate that the ACC method can significantly improve the success rate of the detection by (1) reducing the standard deviation of both the target and noise pixels, and (2) enlarging the separation between feature clusters in color space.

ACKNOWLEDGMENT

We thank the staff of GTRI Food Processing Division for helps in vision hardware. Birds used in these experiments were provided by Gold Kist Inc.

REFERENCES

- [1] D. F. Britton, W. D. Daley, and B. Galloway, "Vision-based citrus inspection and grading system," *Proc. Global Int. Signal Processing Conf.*, Dallas, TX, March 2003.
- [2] W. D. Daley, A Methodology for the Development of Machine Vision Algorithms through the Use of Human Visual Models, PhD thesis, School of Mechanical Engineering, Georgia Inst. of Tech., 2004.
- [3] Q. Li and K.-M. Lee, "Effects of color characterization on computational efficiency of feature detection with live-object handling applications," Submitted to the *IEEE/ASME AIM2005*, Monterey, CA, July 24-28, 2005.
- [4] S. H. Schwartz, *Visual perception: A clinical orientation*. 2nd ed., Appleton & Lance, 1999.
- [5] D. Marr, *Vision: A computational investigation into the human representation and processing of visual information*. W. H. Freeman and Company, New York, 1982.
- [6] T. J. Doll, R. J. Shelton, A. D. Sheffer, C. K. Chiu, M. C. Hetzler, M. K. Higgins, A. A. Wasilewski, N. L. Faust, D. E. Schmieder, and S. E. Glidewell, *Development of an automated multi-spectral image interpretability rating system*. Final Report: Contract No. 00-Z6154-40125 with Eastman Kodak Company, Rochester, NY, October 2000.
- [7] R. Gershon, "The Use of Color in Computational Vision," PhD thesis, Department of Computer Science, University of Toronto, 1987.
- [8] K. Belkacem-Boussaid and A. Beghdadi, "A new image smoothing method based on a simple model of spatial processing in the early stages of human vision," *IEEE Trans. on Image Processing*, 9(2):220.226, February 2000.
- [9] S. Shah and M. D. Levine, "Visual information processing in primate cone pathways-Part I: A model." *IEEE Trans. on Systems, Man, and Cybernetics (T-SMC)-Part B: Cybernetics*, 26(2):259.274, April 1996.
- [10] S. Shah and M. D. Levine, "Visual information processing in primate cone pathways-Part II: Experiments," *IEEE T-SMC-Part B: Cybernetics*, 26(2):275.289, April 1996.
- [11] T. V. Papathomas, R. S. Kashi, and A. Gorea, "A human based computational model for chromatic texture segregation," *IEEE T-SMC*, Part B, 27(3):428.440, June 1997.
- [12] Claudio M. Privitera and Lawrence W. Stark, "Human-vision-based selection of image processing algorithms for planetary exploration," *IEEE Trans. on Image Processing*, 12(8):917.923, August 2003.
- [13] H. Helson, "Fundamental principles in color vision, i - the principle governing changes in hue, saturation, and lightness of non-selective samples in chromatic illumination," *J. of Experimental Psychology*, 23:439-471, 1938.
- [14] D. H. Brainard and B. A. Wandell, "Asymmetric color matching: How color appearance depends on the illuminant," *J. Optical Society of America*, 9:1433-1448, 1992.
- [15] S. W. Kuffler, "Discharge patterns and functional organization of mammalian retina," *J. Neurophysiol.*, 16:37-68, 1953.
- [16] P. Lennie, "Parallel visual pathways: a review," *Vision Res.* 20, 561-594.
- [17] Christina Enroth-Cugell and John Robson, "Functional characteristics and diversity of cat retinal ganglion cells," *Investigative Ophthalmology and Visual Science*, 25:250.267, 1984.
- [18] E. Hering, *Outlines of a Theory of Light Sense*, (translated by Hurvich & Jameson), Cambridge, MA: Harvard U. Press, 1964 (orig. 1920).
- [19] D. K. Reilly, L. N. Cooper, and C. Elbaum, "A Neural Model for Category Learning," *Biological Cybernetics*, Vol. 45, pp35-41, 1982.
- [20] K.-M Lee, J. Joni and X Yin, "Imaging and Motion Prediction for an Automated Live-Bird Transfer Process," *Proc. of the ASME IMECE DSC* November 5-10, Orlando. 2000.
- [21] C. Burges, "A tutorial on support vector machines for pattern recognition," *Data Mining & Knowledge Discovery*, Vol. 2, pp. 121, 1998.